Journal Title
XX(X):1–13

DOI: 10.1177/ToBeAssigned
www.sagepub.com/
SAGE

On the use of stochastic Bouc-Wen model for simulating viscoelastic internal variables from a finite element approximation of steady-rolling tire

Rafael da S. Raqueti [1], Rafael de O. Teloli [2], Samuel da Silva [1], Philippe Bussetta [3], Americo Cunha Jr. [4]

Abstract

Reducing tire rolling resistance and energy loss is a topic of interest to the tire industry. Understanding and modeling these phenomena are essential to approach this problem and propose robust solutions. This work suggests a reduced-order model based on the Bouc-Wen model to simulate internal variables from viscoelastic constitutive laws. Furthermore, sensitivity analysis is performed on the Bouc-Wen parameters to evaluate their influence on the system response and capture the full range of possible values that improve the predictive ability of the reduced-order model. This task is accomplished by calculating the Sobol's indices estimated from a Polynomial-Chaos expansion. Once the range of feasible model solutions is established, the reduced-order model is calibrated through Bayesian inference. Finally, the uncertainties are propagated, and the reduced-order model is validated using data of viscoelastic internal variables from the finite element approximation of a steady-rolling tire. Satisfactory results are obtained, as the reduced-order model can simulate viscoelastic internal variables with a reduced computational cost for some branches of interest. Its responses are in agreement with the experimental data.

Keywords

Viscoelastic internal variables, Bouc-Wen hysteresis model, Sobol' indices, Bayesian inference, Propagation of uncertainties

Introduction

Nowadays, it is necessary to improve sustainable practices in both academic and productive sectors to reduce environmental impacts. Due to the rise of the sustainability mindset in businesses, state regulations, and consumer requirements, the automobile industry has sought to develop technologies aiming to improve vehicle performance, minimize fuel consumption and reduce pollutant emissions. In addition, with the increase in the electric vehicle fleet, the participation of particulate matter generated from brakes and tire wear in pollutant emissions has become important (Oroumiyeh and Zhu 2021; Tonegawa and Sasaki 2021). In this context, improving tire performance is also fundamental.

In a rolling tire, the mechanisms of energy loss have been known for a long time: the hysteresis within the viscoelastic material, the friction between tire and road, and the drag force (Walter and Conant 1974). All these mechanisms of energy loss contribute to the tire rolling resistance, which can be considered as a force that opposes the vehicle motion and is responsible for a significant amount of fuel energy consumption (Hall and Moreland 2001). Most of the rolling resistance is due to hysteresis loss, which depends on the construction of the tire, its material, and external variables such as vehicle speed, wheel load, inflation pressure, etc. (Walter and Conant 1974). Currently, the tire industry is still working on new solutions to reduce the rolling resistance while also improving other tire performance, e.g., improving handling, grip, comfort, and durability, and reducing wear noise. To achieve this, it is crucial to modify the factors that affect the rolling resistance, and it is not worth designing a new tire, doing some tests, and repeating this procedure. Therefore, a robust tire model can be helpful to investigate how the uncertainties in tire properties affect the rolling resistance in the model by increasing or decreasing its value.

In the literature, there are several approaches to model a tire. Pacejka (2012) categorizes these approaches into four types: experimental data only, similarity methods, and simple and complex physical models. The finite element method considers physical complexities and is commonly adopted by the tire industry for modeling the rolling motion (Ghoreishy 2008). The article of Le Tallec and Rahler (1994) is an

[1] UNESP - São Paulo State University, Mechanical Engineering Department, Ilha Solteira, SP, Brazil;
[2] Univ. Bourgogne Franche-Comté, FEMTO-ST Institute, CNRS/UFC/ENSMM/UTBM, Department of Applied Mechanics, 24 chemin de l'Epitaphe, 25000 Besançon, France.
[3] Michelin - Manufacture Française des Pneumatiques Michelin - Clermont Ferrand, France;
[4] UERJ - Rio de Janeiro State University, Rio de Janeiro, RJ, Brazil.

Corresponding author:
Rafael da S. Raqueti, UNESP - São Paulo State University, Mechanical Engineering Department, Av. Brasil 56, 15385-000, Ilha Solteira, SP, Brazil.

Email: rafael.raqueti@unesp.br.

example of the finite element approximation of a pneumatic tire in a steady-state rolling motion. Viscoelasticity is described by constitutive laws, which are internal variables whose evolution is governed by nonlinear differential equations. Nowadays, it is still challenging to characterize the viscoelastic material considering its particularities, such as time-varying properties and energy dissipation. Even with good results, the finite element method can be time-consuming, and the high computational cost motivates the investigation of alternative modeling methods, e.g., the article of Brancati et al. (2011) develops an analytical model of dissipated energy based on a hysteresis model.

Due to model complexity and the presence of nonlinearities in structural dynamics problems such as the viscoelasticity in the modeling of the tire, it is worth analyzing the construction of reduced-order models as an alternative to the complete numerical model (full-order model) to reduce computational time while retaining model accuracy (Sullivan et al. 2022). Unlike the surrogate models based on the definition of response surface (Alizadeh et al. 2020), the reduced-order model is based on physical simplifications of the complete numerical model and depends on the influential parameters that translate these simplifications. The computational time is reduced, and some physical aspects of the complete model are preserved. In this sense, the present work simulates viscoelastic internal variables by solving a computationally less-expensive reduced-order model. Such a model is constructed based on these variables' hysteretic behavior, saving computational time with minor loss of information concerning the full-order finite element model. One of the problems encountered in Bouc-Wen parameter optimization lies in finding sets of parameters that perform similarly. Thus, regarding the parameter identification scheme to compute the Bouc-Wen parameters, a sensitivity analysis is first conducted to establish the full range of feasible model solutions. This paves the way for inferring the reduced-order model parameters via Bayesian inference, gathering knowledge from the available data of the full-order model. This approach's great advantage is obtaining a representative but straightforward model to describe the hysteresis effect in tires within the Bayesian framework. Although this paper addresses the rolling tire problem, the reduced-order model and its parameter calibration strategy can be extended to other systems that involve hysteresis and are computationally expensive to run with finite element models, such as jointed structures (Teloli et al. 2021, 2022; Miguel et al. 2022) and bit-rock interaction of a drill (Real et al. 2019).

Towards this background, the paper is organized as follows: firstly, a problem statement is established. Then, the dataset containing the right Cauchy–Green deformation tensor and viscoelastic internal variables data from the finite element approximation of a steady-rolling tire is introduced. Next, a reduced-order model is suggested to approximate the hysteretic behavior of the viscoelastic internal variables based on the Bouc-Wen model. Then, the methodologies to infer the parameters of the reduced-order model from the dataset and perform a sensitivity analysis are presented. The results of this work are investigated by comparing the responses of the reduced-order model to the viscoelastic internal variables from the dataset. Finally, conclusions, contributions, and perspectives for future inquiry are addressed.

Problem Statement

This work aims to simulate viscoelastic internal variables from a computationally expensive finite element approximation using a reduced-order model, which, in turn, is less computationally expensive to evaluate at first but with an accuracy penalty. Data of viscoelastic internal variables from a finite element approximation of a steady-rolling tire is used. To face this problem, the Methodology of this work is structured as follows:

- First, the reduced-order model and an error measure to evaluate the difference between the reduced-order model responses and viscoelastic internal variables data are defined;
- Second, a global sensitivity analysis is performed to identify the parameters of the reduced-order model that influence the error measure the most. The sensitivity analysis is performed using Sobol' indices, and the parameters whose Sobol' indices are negligible are considered as constant quantities;
- Third, Bayesian inference is performed to calibrate the parameters of the reduced-order model that influence the error measure the most;
- Finally, uncertainties are propagated into both error measure and reduced-order model responses.

The reduced-order model is less computationally expensive, and obtaining viscoelastic internal variables becomes simpler than a finite element procedure involving nonlinear equations.

The Full-Order Model

It is important to stress that the complete development of the finite element model of the tire under analysis is beyond the scope of this work. Confidentiality terms protect further details of material properties, dimensions, and geometry. Nevertheless, this section aims to overview the finite element model addressed. The dataset is generated during the computation of a finite element approximation of a pneumatic tire in a steady rolling motion. A standard procedure approximates the continuous problem by coupling the equilibrium equations governing the steady rolling motion and the constitutive laws governing the viscoelastic material behavior (Le Tallec and Rahler 1994). Due to the nonlinear differential equations that govern the evolution of internal variables, convenient choices of internal variables should be made in terms of differential operators during this standard finite element procedure. Fancello et al. (2006) provide a general framework for constitutive viscoelastic models in which the elastic and viscous potentials derive from a generalized Kelvin-Maxwell model. Le Tallec and Rahler (1994) describe viscoelasticity by choosing the specific free energy potential as a function of three state variables: temperature, right Cauchy-Green deformation tensor, and viscoelastic internal variables. In short, the dataset covered here gathers data from two of these state variables: the right Cauchy-Green deformation tensor C

and the viscoelastic internal variables A form a generalized Maxwell model. The viscoelastic internal variables A are rank 2 symmetric positive-definite tensors (Le Tallec and Rahler 1994).

The theoretical representation of the generalized Maxwell model consists of the parallel association of various Maxwell branches. In addition, each Maxwell branch consists of the series association of elastic and viscous elements. Figure 1 is a general representation of this viscoelastic constitutive model, in which C is the right Cauchy-Green tensor and A_b the viscoelastic internal variables in a Maxwell branch b. The complete numerical model is defined as a generalized Maxwell model containing $N = 10$ Maxwell branches. By analyzing the dataset, it was found that there is no dynamic behavior in the higher order branches. For this reason, the branches of interest in this work are the Maxwell branches from $b = 1$ to 4 in Fig. 1.

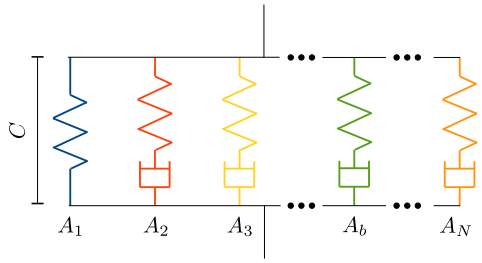

Figure 1. The complete numerical model is the generalized Maxwell model containing $N = 10$ Maxwell branches. The branches of interest are those from $b = 1$ to 4.

The Reduced-Order Model

For one of the branches of interest in Fig. 1, the component $C = C(t)$ of the right Cauchy-Green deformation tensor and its corresponding viscoelastic internal variable $A = A(t)$ are both time series. Therefore, $C(t)$ is assumed to be the sum of three terms: a linear elastic term $k\,A(t)$ in which k is a elasticity coefficient; a viscous term $c\,\dot{A}(t)$ in which c is a damping coefficient; and the hysteresis output $\mathcal{Z}(t)$. In this work, $\mathcal{Z}(t)$ is represented by the Bouc-Wen model. A survey on the Bouc-wen model can be found in Ismail et al. (2009).

The system of first order differential equations in Eq. 1 defines the reduced-order model:

$$\begin{cases} \dot{A}(t) = \dfrac{1}{c}\big(C(t) - k\,A(t) - \mathcal{Z}(A,\dot{A})\big) \\ \dot{\mathcal{Z}} = \alpha\,\dot{A} - \gamma\,|\dot{A}||\mathcal{Z}|^{\nu-1}\mathcal{Z} - \delta\,\dot{A}|\mathcal{Z}|^{\nu}, \end{cases} \tag{1}$$

where the input $C(t)$ is completely determined from the dataset*. For certain initial conditions, $A|_{t=0} = A_0$ and $\mathcal{Z}|_{t=0} = \mathcal{Z}_0$, the output responses $A(\boldsymbol{\theta})$ and $\mathcal{Z}$ depend only on the set of parameter $\boldsymbol{\theta} = \{c, k, \alpha, \gamma, \delta, \nu\}$; the α, γ, δ and ν are the parameters of the Bouc-Wen model. Eq. 1 can be solved numerically by a classic Runge-Kutta method.

Both damping c and elasticity k coefficients are strictly positive parameters. It is worth noting that the Bouc-Wen model is phenomenological, and its parameters α, γ, δ, and ν do not necessarily have a physical sense. Ismail et al. (2009) indicate conditions on the Bouc-Wen model parameters for physical and mathematical consistency, e.g., the Bouc-Wen model fulfills the second law of Thermodynamics if and only if $\nu > 0$, $\gamma > 0$ and $-\gamma \leq \delta \leq \gamma$. Moreover, the Bouc-Wen model is bounded input-bounded output stable and consistent with the motion of physical systems if $\alpha > 0$, $\gamma + \delta > 0$ and $\gamma - \delta \geq 0$. Such parameter conditions are adopted in the calibration methodology to ensure model consistency. Therefore, the following section presents a high-level overview of the methods that are contained in the identification framework proposed.

The Parameters Calibration Methodology

The Bouc-Wen model has the advantage of accommodating real hysteresis loops by choosing an appropriate set of parameters (Ismail et al. 2009). For this reason, problems involving the Bouc-Wen model are typically parameter estimation problems, as the example described in Jiang et al. (2020).

A representative set containing several inputs is selected from the dataset (due to the formulation of the right Cauchy-Green tensor, the same setting is applied to all branches). In this single set, the inputs differ from each other in maxima and minima values, derivatives, etc. A logical approach is to identify a reduced-order model for each of these inputs in a branch of interest. However, this would substantially increase the complexity of the problem and the number of parameters to be identified. Therefore, the strategy adopted by this work lies in defining a unique reduced-order model that best forecasts viscoelastic internal variables for a branch of interest considering the whole set of different inputs. To compare the discrepancies between the outputs of the reduced-order model with the internal viscoelastic variables independently of inputs, an error measure that evaluates these differences is defined.

Equation 2 defines the scale factor $\bar{A}$, where A^{DS} is a viscoelastic internal variable from the dataset and N_{out} is the number of sampling points of the time series:

$$\bar{A} = \frac{1}{N_{\text{out}} - 1}\sum_{l=2}^{N_{\text{out}}} \big|\big|A_l^{\text{DS}} - A_{l-1}^{\text{DS}}\big|\big|, \tag{2}$$

and Eq. 3 defines E, the mean absolute scaled error (MASE) that measures the difference between the selected output A^{DS} from the dataset and $A(\boldsymbol{\theta})$:

$$E(\boldsymbol{\theta}) = \frac{1}{N_{\text{out}}}\sum_{l=1}^{N_{\text{out}}} \frac{\big|\big|A_l^{\text{DS}} - A_l(\boldsymbol{\theta})\big|\big|}{\bar{A}}. \tag{3}$$

Hyndman and Koehler (2006) suggests that the MASE is the best available measure of forecast accuracy in situations where there are very different scales, including close to zero or negative data. Equation 4 is simply the mean between the N_{in} error measures, where each $E_j(\boldsymbol{\theta})$ corresponds to the evaluation of a reduced-order model response:

$$\bar{E}(\boldsymbol{\theta}) = \frac{1}{N_{\text{in}}}\sum_{j=1}^{N_{\text{in}}} E_j(\boldsymbol{\theta}). \tag{4}$$

*This parameter is assumed to be an input variable in the model and is therefore known for the whole range of analysis

Equation 4 also defines the loss function of an optimization problem. The optimal solution of this optimization problem is indicated in Eq. 5:

$$\hat{E} = \bar{E}(\hat{\boldsymbol{\theta}}), \quad \hat{\boldsymbol{\theta}} = \arg\min_{\mathcal{B}} \bar{E}(\boldsymbol{\theta}), \tag{5}$$

where $\hat{\boldsymbol{\theta}}$ is the optimal set of parameter in the set of feasible solutions $\mathcal{B}$ that minimizes the error measure between the selected viscoelastic internal variables A^{DS} from the dataset and the reduced-order model responses $A(\boldsymbol{\theta})$. After introducing a metric capable of assessing the performance of the reduced model, the next subsection introduces the global sensitivity analysis for evaluating the Bouc-Wen parameters.

Each of the following methods has its canonical notation in the literature. The continuation of this paper respects these canonical notations, and redundancies may be related to this.

Global sensitivity analysis and PCE-based Sobol' indices

Global sensitivity analysis (GSA) refers to a set of mathematical techniques that quantifies the influence of the input parameters on the response of interest of a system. The GSA can be defined among other techniques by the variance decomposition method, which aims to decompose the output variance as the sum of each input variable's contributions or combinations. Sobol' indices is a variance decomposition method defined in Sobol (1993) that engineers have recently explored. Its central idea is to determine the expansion of a computational model into the sum of increasing dimensions and the rapport of the partial variances of these terms concerning the model's total variance.

Generally speaking, let $\mathcal{M}$ be a mathematical model and $\boldsymbol{X}$ a random input vector gathering k independent input parameters. $\mathcal{M}$ describes a scalar output of interest Y of a physical system:

$$Y = \mathcal{M}(\boldsymbol{X}) \quad , \quad \boldsymbol{X} = \{X_1, X_2, \ldots, X_k\}\,. \tag{6}$$

According to Sobol (1993), Y can be defined by the decomposition into sums of different dimensions. For simplification purposes, the following equations will assume that the input parameters are uniformly distributed and the support of $\boldsymbol{X}$ is $\mathcal{D}_{\boldsymbol{X}} = [0,1]^k$. Therefore, Y can be also written as:

$$Y = \mathcal{M}_0 + \sum_{i=1}^{k} \mathcal{M}_i\left(X_i\right) + \sum_{i<j}^{k} \mathcal{M}_{ij}\left(X_i, X_j\right) + \ldots + \mathcal{M}_{1\ldots k}\left(X_1 \ldots X_k\right). \tag{7}$$

All terms of this expansion can be computed through integrals. The first term $\mathcal{M}_0$ is a constant equal to the expected value:

$$\mathcal{M}_0 = \int_{\mathcal{D}_{\boldsymbol{X}}} \mathcal{M}\left(\boldsymbol{X}\right)\, d\boldsymbol{X}. \tag{8}$$

The other terms $\mathcal{M}_i(X_i)$ and $\mathcal{M}_{ij}(X_i, X_j)$ are the conditional mean values for the parameters i and ij $(i \neq j)$, respectively:

$$\mathcal{M}_i(X_i) = \int_0^1 \cdots \int_0^1 \mathcal{M}\left(\boldsymbol{X}\right)\, d\boldsymbol{X}_{\sim i} - \mathcal{M}_0, \tag{9}$$

$$\mathcal{M}_{ij}(X_i, X_j) = \int_0^1 \cdots \int_0^1 \mathcal{M}\left(\boldsymbol{X}\right)\, d\boldsymbol{X}_{\sim ij} - \mathcal{M}_0 - \mathcal{M}_i(X_i) - \mathcal{M}_j(X_j). \tag{10}$$

The notation $\sim i$ indicates that parameter X_i is excluded. Eq. 7 has the property of orthogonality in terms of conditional means as defined by Homma and Saltelli (1996), and it is possible to define the Sobol decomposition in terms of conditional variances (Sobol 1993). Thus, one can compute the first-order Sobol's indices that quantify the additive effect of each input parameter separately concerning the total variance:

$$S_i = \frac{Var[\mathcal{M}_i(X_i)]}{Var[\mathcal{M}(\boldsymbol{X})]}, \tag{11}$$

and the second-order Sobol' indices that quantify the interaction effects between two input parameters:

$$S_{ij} = \frac{Var[\mathcal{M}_{ij}(X_i, X_j)]}{Var[\mathcal{M}(\mathbf{X})]}. \tag{12}$$

Higher-order Sobol' indices are equally defined, and they take into account the interaction effects of various input parameters.

Monte Carlo simulation can compute Sobol's indices, although it has a high computational cost due to the low convergence rate. An alternative way to calculate Sobol's indices is constructing a surrogate model based on Polynomial-Chaos Expansion (PCE), which reduces the processing time and computational cost while maintaining model accuracy. Applications of the PCE for computing the Sobol' indices can be seen in Crestaux et al. (2009) and Palar et al. (2018) and Sudret (2008) presents a review on GSA using PCE.

Based on PCE expression, the scalar output of interest Y can be rewritten as:

$$Y \approx \sum_{\alpha \in \mathcal{A}} y_\alpha \psi_\alpha(X), \tag{13}$$

where ψ_α represents multivariate polynomials that are orthonormal in relation to the joint probability density function $f_{\boldsymbol{X}}$, y_α are unknown deterministic coefficients and $\mathcal{A}$ is a truncation criterion, where $\mathcal{A} \subset \mathbb{N}^M$ is the set of selected multi-indices of multivariate polynomials. The coefficients can be determined through the least angle regression method.

The statistics of an uncertain output response Y can be determined using PCE. Therefore, the mean and the variance are defined, respectively, by:

$$\mathcal{M}_0 = y_0 \quad \text{and} \quad \widehat{Var}(Y) = \sum_{\alpha \in \mathcal{A}} y_\alpha^2. \tag{14}$$

Therefore, the Sobol indices can be directly determined with minor computational effort through the PCE coefficients. Thus, the first and second-order Sobol' indices are, respectively:

$$S_i^{PCE} = \sum_{\substack{\alpha \in \mathcal{A}_i \\ \alpha \neq 0}} y_\alpha^2 \Big/ \sum_{\alpha \in \mathcal{A}} y_\alpha^2, \tag{15}$$

$$S_{ij}^{PCE} = \sum_{\substack{\alpha \in \mathcal{A}_{ij} \\ \alpha \neq 0}} y_\alpha^2 \Big/ \sum_{\alpha \in \mathcal{A}} y_\alpha^2. \tag{16}$$

Thus, the Sobol indices are computed via a PCE-based surrogate model to verify the influence of the reduced-order model parameters on the error measure.

The Cross-Entropy method

To verify how uncertainty in the parameters of the reduced-order model propagates into its response through Bayesian inference, a necessary ingredient is to learn the a priori distributions of each parameter. Thus, it is obtained from initial results considering the Cross-Entropy (CE) method as an optimization procedure for minimizing the objective function 5.

The CE method translates a rare event simulation problem into an optimization problem, and this method can be treated as a two-step iterative process:

- First, random samples are generated according to a given probability distribution is determined feasible region;
- Then, the statistics, i.e., the mean and variance of a set composed of the best performing samples, are used to refine the probability distribution parameters.

Among other applications, the CE method can be used to solve continuous optimization and combinatorial optimization problem (De Boer et al. 2005). Additional information about its theoretical framework and practical considerations about the optimization method can be found in Rubinstein and Kroese (2013).

The central idea of the CE method is based on importance sampling technique and variance minimization. At first, let $X \sim f$ be a random variable with probability density function (PDF) f and let $H(X)$ be a function. The expected value of $H(X)$ is:

$$\mu_f = \mathbb{E}_f\{H(X)\} = \int_{\mathcal{B}} H(x) f(x) dx. \tag{17}$$

Let g also be a PDF. The expected value of $H(X)\frac{f(X)}{g(X)}$ is:

$$\mu_g = \mathbb{E}_g\Big\{H(X)\frac{f(X)}{g(X)}\Big\} = \int_{\mathcal{B}} H(x)\frac{f(x)}{g(x)} g(x) dx. \tag{18}$$

The importance sampling estimator $\hat{\mu}_g$ is:

$$\hat{\mu}_g = \frac{1}{N_k}\sum_{k=0}^{N_k} H(x_k)\frac{f(x_k)}{g(x_k)}, \quad X \sim g, \tag{19}$$

where the term on the right defines $W(x) = \frac{f(x)}{g(x)}$ the likelihood ratio. The quality of the estimator $\hat{\mu}_g$ depends on the PDF g. The optimal importance sampling PDF $\hat{g}^*$ is the one in which the variance of $\hat{\mu}_g$ is minimal.

The Kullback-Leibler divergence denoted $\mathcal{D}(g, h)$ offers a measure of how different a chosen PDF h is with respect to the reference PDF g. It is defined as follows in Eq. 20:

$$\mathcal{D}(g, h) = \mathbb{E}_g\Big\{\ln\frac{g(X)}{h(X)}\Big\}. \tag{20}$$

The PDF $f(\cdot; \boldsymbol{v})$ determined by the hyper-parameters vector $\boldsymbol{v}$ is chosen. As it is shown in Kroese et al. (2013), the minimization of $\mathcal{D}(\hat{g}^*, f(\cdot, \boldsymbol{v}))$ leads to Eq. 21, with $\hat{g}^* \propto Hf(\cdot; \boldsymbol{u})$:

$$\boldsymbol{v}^* = \arg\max_{\boldsymbol{w}} \mathbb{E}_{\boldsymbol{w}}\Big\{H(x)W(x; \boldsymbol{u}, \boldsymbol{w}) \ln f(x; \boldsymbol{v})\Big\}. \tag{21}$$

Finally, for $X_s \sim f(\cdot; \boldsymbol{w})$ and $W(x_s; \boldsymbol{u}, \boldsymbol{w}) = \frac{f(\cdot; \boldsymbol{u})}{f(\cdot; \boldsymbol{w})}$, $\hat{\boldsymbol{v}}$ is the hyper-parameter vector that approximates to the optimal importance estimator (minimal variance):

$$\hat{\boldsymbol{v}} = \arg\max_{\boldsymbol{w}} \frac{1}{N_k}\sum_{k=0}^{N_k} H(x_k)W(x_k; \boldsymbol{u}, \boldsymbol{w}) \ln f(x_k; \boldsymbol{v}). \tag{22}$$

Some assumptions are made in the sequence about the function $H(x)$. For rare event simulation and optimization problems, $H(x) = \mathbb{1}_{J(x)\geq\epsilon}$ where $\mathbb{1}_{J(x)\geq\epsilon}$ is the indicator function and $J(x)$ is an objetive function. Specifically, in this work:

$$H(\boldsymbol{\theta}) = \mathbb{1}_{\bar{E}(\boldsymbol{\theta})\geq\epsilon} = \begin{cases} 1 & \text{if } \bar{E}(\boldsymbol{\theta}) \geq \epsilon \\ 0 & \text{if } \bar{E}(\boldsymbol{\theta}) < \epsilon. \end{cases} \tag{23}$$

The expected value of the indicator function is the probability of the event $\bar{E}(\boldsymbol{\theta}) \geq \epsilon$ to occur.

$$\mu = \mathbb{E}\{\mathbb{1}_{\bar{E}(\boldsymbol{\theta})\geq\epsilon}\} = \mathcal{P}\{\bar{E}(\boldsymbol{\theta}) \geq \epsilon\}, \tag{24}$$

and its importance sampling estimator $\hat{\mu}_g$ is:

$$\hat{\mu}_g = \frac{1}{N_k}\sum_{k=0}^{N_k} \mathbb{1}_{\bar{E}(\boldsymbol{\theta}^{(k)}))\geq\epsilon}. \tag{25}$$

Cunha (2021) intuitively describes the computational algorithm of the CE method through the following steps:

1. **Initialize:** Choose initial hyper-parameters values $\hat{\mu}_0$ and $\hat{\sigma}_0^2$, and $\hat{\boldsymbol{v}}_0 = \{\hat{\mu}_0, \hat{\sigma}_0^2\}$. Set level counter $l = 1$;
2. **Sampling:** Generate N_k independent and identically distributed (iid) samples from the standard multivariate Gaussian distribution:
$$\boldsymbol{\theta}^{(1)}, \ldots, \boldsymbol{\theta}^{(N_k)} \sim \mathcal{N}\big(\hat{\mu}_{l-1}, \hat{\sigma}_{l-1}^2\big);$$
3. **Select:** Evaluate the objective function for each sample and sort the N_k results in order:
$$\bar{E}(\boldsymbol{\theta}^{(\cdot)}) \leq \cdots \leq \bar{E}(\boldsymbol{\theta}^{(\cdot)}).$$
The called elite sample set $\mathcal{E}$ gathers the $N_\mathcal{E} < N_k$ samples that better performed;
4. **Update:** Compute estimators:
$$\tilde{\mu}_l = \frac{1}{N_\mathcal{E}}\textstyle\sum_{s=1}^{N_\mathcal{E}} \boldsymbol{\theta}^{(s)} \tag{26}$$
$$\hat{\sigma}_l^2 = \frac{1}{N_\mathcal{E}}\textstyle\sum_{s=1}^{N_\mathcal{E}} \big(\boldsymbol{\theta}^{(s)} - \tilde{\mu}_l\big)^2; \tag{27}$$
5. **Smooth:** Apply the smooth updating schema:
$$\hat{\mu}_l := a \cdot \tilde{\mu}_l + (1 - a) \cdot \hat{\mu}_{l-1}; \tag{28}$$
6. **Return** $\hat{\boldsymbol{\theta}} = \hat{\mu}_l$ if the stopping criteria $\hat{\sigma}_l^2 < \epsilon_{\text{max}}$ is reached. Otherwise, increase level counter by 1 and return to the second step.

Operationally, the hyper-parameters vector $\hat{\boldsymbol{v}}$ in Eq. 22 can be estimated via maximum likelihood estimation method. The use of the standard multivariate Gaussian distribution (Botev 2016) on the sampling step of the CE method simplifies the estimation of $\hat{\boldsymbol{v}}$ and the hyper-parameters can be computed directly by Eqs. 26 and 27.

Despite its mathematical formulation, the CE method can be easily implemented, and only few parameters that are pretty intuitive are needed: given the PDF $f(\cdot;\boldsymbol{v})$, the total number of samples N_s, the number of samples $N_{\mathcal{E}}$ in the elite sample set, a stopping criterion $\epsilon_{\max}$ and the maximum of iteration level $l_{\max}$.

To the sequence, $\hat{E}$ can be computed using Eq. 5 and the parameters of the reduced-order model are considered as random quantities. Their distributions are inferred via Bayesian inference.

Bayesian inference

Bayesian inference approach is a straightforward strategy to quantify uncertainties (Gelman et al. 2013). A set of parameter is considered as a random input vector $\boldsymbol{x}$ and the methodology to infer its distribution is based on the Bayes' theorem in Eq. 29:

$$\pi(\boldsymbol{x}|\hat{\boldsymbol{E}}) = \frac{\pi(\hat{\boldsymbol{E}}|\boldsymbol{x})\,\pi(\boldsymbol{x})}{\pi(\hat{\boldsymbol{E}})}, \tag{29}$$

where $\pi(\boldsymbol{x})$ is the prior distribution of the set of parameters $\boldsymbol{x}$; $\pi(\hat{\boldsymbol{E}}|\boldsymbol{x})$ is the likelihood function of $\hat{\boldsymbol{E}}$ given a set of parameters $\boldsymbol{x}$ at hand; and $\pi(\boldsymbol{x}|\hat{\boldsymbol{E}})$ is the posterior distribution of the set of parameters $\boldsymbol{x}$ given $\hat{\boldsymbol{E}}$. The denominator $\pi(\hat{\boldsymbol{E}})$ is the marginal likelihood: it is a normalized constant so the posterior distribution defines a probability density function with integral equal to the unity. In this case, Eq. 29 can be simplified into:

$$\pi(\boldsymbol{x}|\hat{\boldsymbol{E}}) \propto \pi(\hat{\boldsymbol{E}}|\boldsymbol{x})\,\pi(\boldsymbol{x}). \tag{30}$$

The prior distribution $\pi(\boldsymbol{x})$ can be interpreted as the knowledge degree about $\boldsymbol{x}$ before any evidence. It is classified based on its influence on the posterior distribution, and an example of a diffuse – or non-informative – prior is a Uniform prior distribution. In this case, Eq. 30 can also be simplified into:

$$\pi(\boldsymbol{x}|\hat{\boldsymbol{E}}) \propto \pi(\hat{\boldsymbol{E}}|\boldsymbol{x}). \tag{31}$$

One assumes that $\hat{E}$ is the MASE measure $\bar{E}(\boldsymbol{\theta})$ from the reduced-order model plus a discrepancy term $\boldsymbol{\epsilon}$ that is the source of uncertainty:

$$\hat{E} = \bar{E}(\boldsymbol{\theta}) + \epsilon. \tag{32}$$

It is supposed an additive Gaussian discrepancy with mean $\mu_\epsilon = 0$ and unknown variance σ_ϵ^2. Thus, $\epsilon \sim \mathcal{N}(0, \sigma_\epsilon^2)$ and:

$$\pi\big(\hat{E}|\boldsymbol{x} = \{\boldsymbol{\theta}, \sigma_\epsilon^2\}\big) \sim \mathcal{N}\big(\hat{E}|\ \bar{E}(\boldsymbol{\theta}), \sigma_\epsilon^2\big). \tag{33}$$

In the case of independent and identically distributed (iid) observations, the likelihood function is defined as:

$$\begin{aligned}\pi\big(\hat{\boldsymbol{E}}|\boldsymbol{x}\big) &= \prod_{i=1}^{N} \pi\big(\hat{E}_i|\boldsymbol{x}\big) \\ &= \frac{1}{\sqrt{2\pi\sigma_\epsilon^2}} \exp\left(-\frac{1}{2} \sum_{i=1}^{N} \frac{\big(\hat{E}_i - \bar{E}(\boldsymbol{\theta})\big)^2}{\sigma_\epsilon^2} \right).\end{aligned} \tag{34}$$

After Eqs. 31 and 34, the posterior distribution can be finally defined as follows:

$$\pi(\boldsymbol{x}|\hat{\boldsymbol{E}}) \propto \frac{1}{\sqrt{\sigma_\epsilon^2}} \exp\left(-\frac{1}{2} \sum_{i=1}^{N} \frac{\big(\hat{E}_i - \bar{E}(\boldsymbol{\theta})\big)^2}{\sigma_\epsilon^2} \right). \tag{35}$$

To determine the posterior distribution $\pi(\boldsymbol{x}|\hat{\boldsymbol{E}})$ of parameters $\boldsymbol{x}$ given $\hat{\boldsymbol{E}}$ is not always trivial. Usually, Monte Carlo simulation is used to approximate the solutions. This book is a review on Monte Carlo methods (Kroese et al. 2011).

The Metropolis-Hastings algorithm is a Markov chain Monte Carlo (MCMC) method based on the construction of a Markov chain such that the future state $\boldsymbol{x}^{(k+1)}$ of the chain depends only on its current state $\boldsymbol{x}^{(k)}$ and a transition probability distribution $\mathcal{T}\big(\boldsymbol{x}^{(k+1)}|\ \boldsymbol{x}^{(k)}\big)$. In the presence of a sufficient number of unbiased samples, the sequence of random variables $\boldsymbol{X} = \{\boldsymbol{x}^{(0)}, \boldsymbol{x}^{(1)}, \boldsymbol{x}^{(2)}, ...\}$ represents the posterior distribution $\pi(\boldsymbol{x}|\hat{\boldsymbol{E}})$.

$$\frac{\pi\big(\boldsymbol{x}^{(k+1)}|\hat{\boldsymbol{E}}\big)}{\pi\big(\boldsymbol{x}^{(k)}|\hat{\boldsymbol{E}}\big)} = \frac{\mathcal{T}\big(\boldsymbol{x}^{(k+1)}|\boldsymbol{x}^{(k)}\big)}{\mathcal{T}\big(\boldsymbol{x}^{(k)}|\boldsymbol{x}^{(k+1)}\big)}. \tag{36}$$

The procedure for generating the future state $\boldsymbol{x}^{(k+1)}$ is a two-stage process: the first stage is to generate a candidate $\boldsymbol{x}^{(*)}$ that depends only on the current state $\boldsymbol{x}^{(k)}$ of the Markov chain; the second stage is to accept or reject $\boldsymbol{x}^{(*)}$. To this end, it is necessary to compute the acceptance probability a according to Eq. 37 where $\mathcal{K}\big(\boldsymbol{x}^{(*)}|\boldsymbol{x}^{(k)}\big)$ is the proposed probability distribution.

$$a = \min\left\{1, \frac{\pi\big(\boldsymbol{x}^{(*)}|\hat{\boldsymbol{E}}\big)\ \mathcal{K}\big(\boldsymbol{x}^{(*)}|\boldsymbol{x}^{(k)}\big)}{\pi\big(\boldsymbol{x}^{(k)}|\hat{\boldsymbol{E}}\big)\ \mathcal{K}\big(\boldsymbol{x}^{(k)}|\boldsymbol{x}^{(*)}\big)}\right\}. \tag{37}$$

Then, a random number $u \sim \mathcal{U}(0,1)$ is generated from a Uniform distribution with parameters 0 and 1. If $u < a$, the candidate $\boldsymbol{x}^{(*)}$ is accepted and $\boldsymbol{x}^{(k+1)} = \boldsymbol{x}^{(*)}$. Otherwise, if $u \geq a$, $\boldsymbol{x}^{(*)}$ is rejected and $\boldsymbol{x}^{(k+1)} = \boldsymbol{x}^{(k)}$.

The random walk Metropolis algorithm is a particular case of the Metropolis-Hastings algorithm. In it, a symmetric Gaussian distribution with variance σ^2 is proposed to generate the candidate $\boldsymbol{x}^{(*)}$ (Saadi et al. 2011) yielding:

$$a = \min\left\{1, \frac{\pi(\boldsymbol{x}^{(*)}|\hat{\boldsymbol{E}})}{\pi(\boldsymbol{x}^{(k)}|\hat{\boldsymbol{E}})}\right\}. \tag{38}$$

The following steps summarizes the random walk Metropolis algorithm:

cInitialize the counter and assign initial value $\boldsymbol{x}^{(0)}$; Generate a candidate $\boldsymbol{x}^{(*)} \sim \mathcal{N}(\boldsymbol{x}^{(k)}, \sigma^2)$; Compute the acceptance probability $a\big(\boldsymbol{x}^{(*)}, \boldsymbol{x}^{(k)}\big)$ and generate a random number $u \sim \mathcal{U}(0,1)$; Does $u < a$? If

positive, accept the candidate and $\boldsymbol{x}^{(k+1)} = \boldsymbol{x}^{(*)}$. If negative, reject and $\boldsymbol{x}^{(k+1)} = \boldsymbol{x}^{(k)}$; Increment the counter and return to the second step.

This article adopted some strategies while implementing the Metropolis-Hastings algorithm to accelerate the convergence of the Markov chain (Saadi et al. 2011). A first feature is the total number of generated samples: the Markov chain must be large enough to adequately represent the distributions of the parameters respecting the law of large numbers. The second one is the acceptance probability rate $\bar{a} = \frac{N_a}{N_k}$ that is the ratio between the number of accepted samples N_a and the total number of generated samples N_k. $\bar{a}$ is controlled by the random walk step σ: on the one hand, if the jump from one sample to the other is too large, $\bar{a}$ is small, and the chain keeps static; on the other hand, if the jump from one sample to the other is too small, $\bar{a}$ is big, and the chain needs more time to go through the parameters space. Saadi et al. (2011) consider an optimal $\bar{a}$ between $40\% - 50\%$. The last feature is the burn-in: eliminating a defined number of initials samples from the final result. This feature is essential to eliminate biased results.

Figure 2 is an overview of the present Methodology for calibrating the reduced-order parameters and simulating viscoelastic internal variables. Instead of applying complex techniques to construct the reduced-order model, the insights of this Methodology are: 1) even treating a complex nonlinear problem such as viscoelasticity, the reduced-order model consists of a simple system of nonlinear differential equations; 2) Sobol' indices evaluate the importance of the parameters, combined or individually, on the variability of the responses. In addition, Sobol's indices justify the necessity to calibrate or not a parameter; 3) The cross-entropy method guarantees convergence; 4) Both the cross-entropy method and the Bayesian inference can be easily implemented. In addition, Sobol' indices can be evaluated using open-sources libraries; 5) The reduced-order model is calibrated using data that originated from a finite element model, the standard model in the tire industry; 6) The same approach used in this paper can be used to solve other structural dynamics problems (e.g., friction models with a population of sliders, such as the Iwan model (Segalman 2005)).

Results and Discussion

The calibration methodology is first applied to the first branch of interest. The same procedure for inferring the parameters of the reduced-order model was adopted for the other branches. It is assumed that each parameter follows a Uniform distribution $\mathcal{U}(a, b)$, with a its minimum and b its maximum value. The limits are chosen so that the Bouc-Wen model is physically and mathematically consistent. The supports are indicated in Tab. 1.

A prior global sensitivity analysis is performed in order to verify which reduced-order model parameter is influential. To do so, a PCE-based surrogate model $\tilde{E}(\boldsymbol{\theta})$ is first built and the PCE coefficients were computed using UQLab metamodeling module based on sparse least angle regression (Marelli et al. 2021). A comparison between responses $\bar{E}(\boldsymbol{\theta})$ and $\tilde{E}(\boldsymbol{\theta})$ can be seen in Fig. 3: the closer to the black diagonal line, the more reliable the PCE-based surrogate model is. In Fig. 3, both $\bar{E}(\boldsymbol{\theta})$ and $\tilde{E}(\boldsymbol{\theta})$ were evaluated at 100 cross-validation sample points. It is worth mentioning that the reduced-order model is not yet calibrated and it is natural to observe in Fig. 3 high error measure values, e.g., $\bar{E}(\boldsymbol{\theta}) > 1$. Table 2 contains additional information about the validation of the PCE-based surrogate model.

Once the PCE-based surrogate model is validated, the Sobol's indices are computed with minor computational efforts. This procedure allows drawing some conclusions about the reduced-order model parameters before inferring their distributions. Figure 4 shows the total and first-order Sobol' indices. On the one side, these results indicate that parameters γ and δ have little influence on the error measure, i.e., having less or more variability on these parameters does not mean that the reduced-order model simulates viscoelastic internal variables more accurately. For this reason, they are considered as completely determined quantities and their values are set to $\gamma = 1000$ and $\delta = 1000$ so $\frac{\gamma}{\gamma+\delta} = 0.5$. On the other side, parameters c, α, k and ν have considerable influence. Their variability requires attention, and they are considered as unknowns.

Next, the optimization problem of Eq. 5 is solved using the CE method. The CE parameters used in this step are $N_s = 100$ samples, $N_{\mathcal{E}} = 4$ samples, $l_{\max} = 500$ iterations and $\epsilon_{\max} = 10^{-6}$. In addition, a smooth updating schema of 0.8 is also used. Table 3 contains the optimal parameters of the reduced-order model of the Branch 1. In this case, $\hat{E} = 0.3168$ and these parameter values can be used for deterministic simulation of viscoelastic internal variables.

However, it is also desirable to verify how the uncertainties propagate into the responses of the reduced-order model. To do this, the parameters c, k, α, ν and the variance σ_ϵ^2 of the discrepancy are first calibrated using Bayesian inference. The following procedure is adopted:

1. The values of a and b of the Uniform prior distribution $\mathcal{U}(a, b)$ were redefined because it was visually verified that the range of values was too wide. The new bounds are indicated in Tab. 4;
2. In an iterative way: a Markov chain containing 10^4 samples were generated. Then, the random walk step σ was manually adjusted so that the acceptance rate was $\bar{a} \approx 40 - 50\%$;
3. After setting an acceptable random walk step value, a Markov chain containing 10^5 samples was generated and retained. No burn-in samples were eliminated.

Figure 5 shows the trace plots of parameters c, k,α,ν and σ_ϵ^2 of Branch 1. In this figure, "Data" corresponds to the 10^5 samples in the Markov chain, and the red lines support the Uniform distribution. The cumulative mean indicates the convergence of the Markov chain. There is no need to eliminate burn-in samples because the optimal parameters of the CE method allow the Markov chain to start in a stable region. Figure 5 also indicates that this Markov chain can be used to determine the distributions of the parameters of the reduced-order model. Moreover, Fig. 6 shows the densities and cumulative densities of each one of these parameters. In this figure, the continuous black lines are the probability density estimates (EPDFs) based on a normal kernel function, and the marked red lines are the empirical cumulative distribution functions (ECDFs). It is interesting

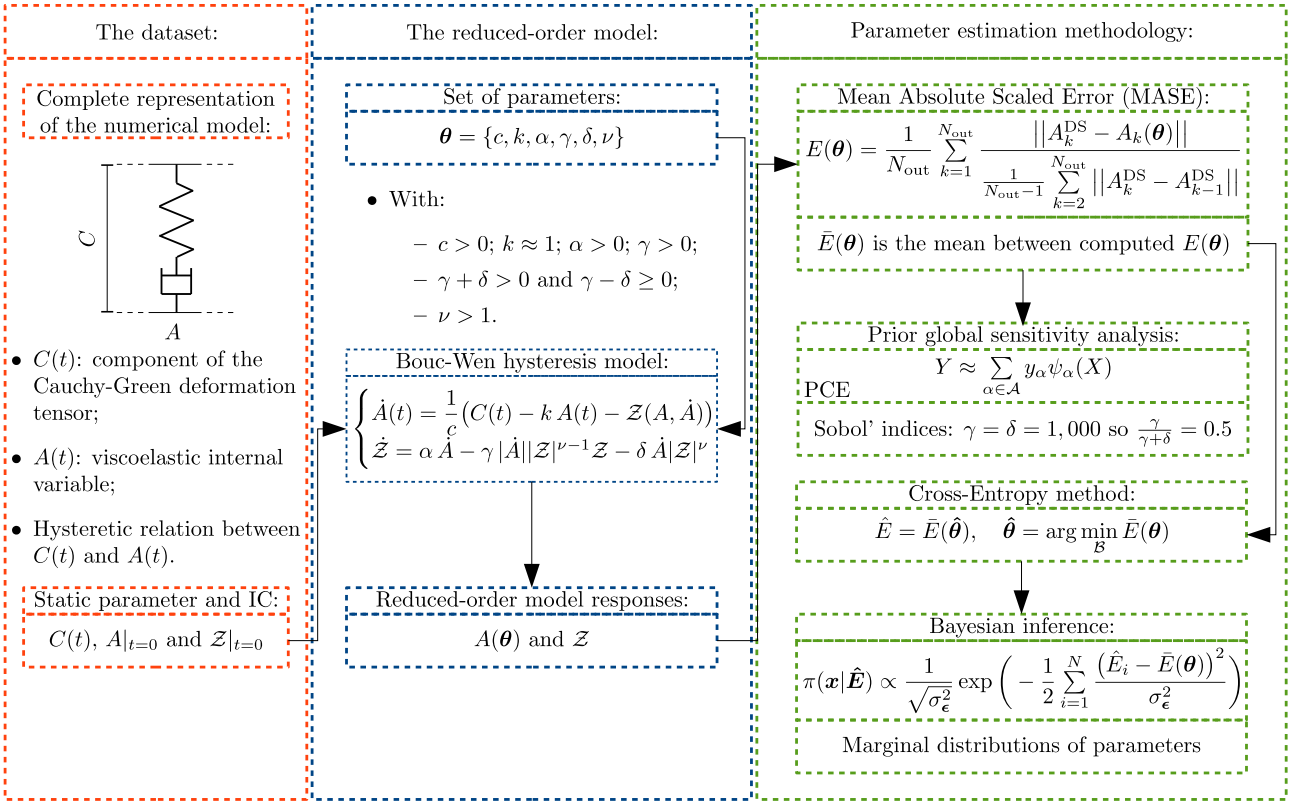

Figure 2. Methodology adopted to simulate viscoelastic internal variables.

Table 1. Uniform prior distribution $\mathcal{U}(a, b)$ of the reduced-order model parameters for global sensitivity analysis.

Support	c	k	α	γ $[\times 10^3]$	δ $[\times 10^3]$	ν
a	0	0.999	0	1	-1	1
b	0.01	1.001	1	10	1	3

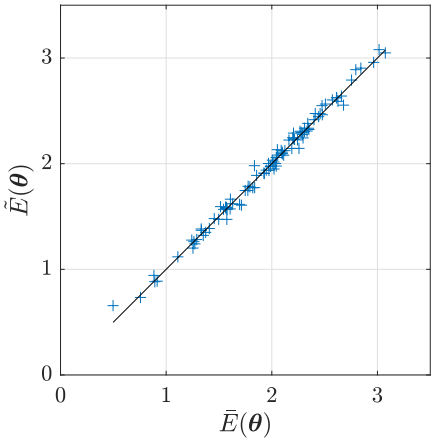

Figure 3. Comparison between responses $\bar{E}(\boldsymbol{\theta})$ and $\tilde{E}(\boldsymbol{\theta})$. The disposition of the 100 cross-validation samples $+$ indicates that the PCE-based surrogate model is adequate.

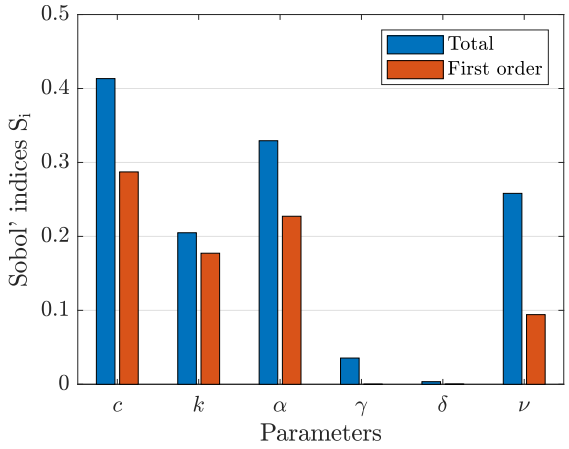

Figure 4. Prior global sensitivity analysis. Total and first order Sobol' indices of parameters γ and δ are negligible. Therefore, they can be considered as determined quantities. Only parameters c, k, α and ν are calibrated.

Table 2. Validation of the PCE-based surrogate model.

PCE degree	Exp. Design	LOO error
14	$2,000$	$5.7 \cdot 10^{-3}$

Table 3. Reduced-order model optimal parameters values given by the CE method.

$\hat{c}$	$\hat{k}$	$\hat{\alpha}$	$\hat{\nu}$
0.0018	1.0000	0.1152	1.0220

to compare the Uniform distributions in black dashed line with the EPDF: the distributions changes from the former to the latter as new information is used to update the Bayesian

inference. From the inferred distributions, some conclusions can be drawn:

- It is possible to notice that the samples are centered around 0.002 and 1 for parameters c and k, respectively;
- There is a higher tendency for parameter α to get values between 0 and 0.2;
- There is a higher tendency for parameter ν to get values close to 1.

Once the distributions of the parameters of the reduced-order model are estimated, it is possible to proceed with the propagation of uncertainties. For each branch of interest, the distributions of the error measures were obtained after performing this propagation. Figure 7 also shows the density and the cumulative density functions of the error measures $E(\boldsymbol{\theta})$. The continuous black lines are the EPDFs based on a normal kernel function and the marked red lines the ECDFs. In addition, the vertical dashed magenta lines indicate the optimal error measures $\hat{E}$, which were determined using the CE method. On the one hand, from the observation of the ECDFs, there is a high probability of having $E(\boldsymbol{\theta}) \leq 1$ in Branches 1 to 3. On the other hand, $\hat{E} > 1$ in Branch 4. Adopting this criterion, the calibrated reduced-order models are suitable for simulating the viscoelastic internal variables of Branches 1 to 3 and less suitable for Branch 4.

Finally, Fig. 8 shows for Branch 1 some of the responses of the reduced-order model with uncertainties. The inputs and initial conditions used to validate the reduced-order model are not the same as those used during the calibration procedure. This figure evidences the good agreement between the reduced-order model responses and the data, as the viscoelastic internal variables of the dataset are within the 95% confidence interval in gray and are also close to the stochastic reduced-order model mean, the dashed black line.

Conclusions

This work suggests a reduced-order model simulating viscoelastic internal variables that describe the behavior of viscoelastic structures. Michelin furnished data on the right Cauchy-Green deformation tensor and viscoelastic internal variables to carry out this work. These data were generated during a finite element-based steady-rolling tire approximation computation.

Rather than solving a physically complex finite element model, an advantage of this reduced-order model is that it simulates viscoelastic internal variables by solving a system of nonlinear differential equations: the suggested reduced-order model is based on the hysteretic behavior between the components of the right Cauchy-Green deformation tensor and viscoelastic internal variables. This system of nonlinear differential equations is simpler to implement numerically, and its computation is less expensive than a finite element model.

An error metric is defined to evaluate the discrepancies between the reduced-order model responses and data. Then, a calibration procedure is proposed based on: 1) performing a global sensitivity analysis by evaluating Sobol' indices from a PCE-based surrogate model; 2) obtaining the

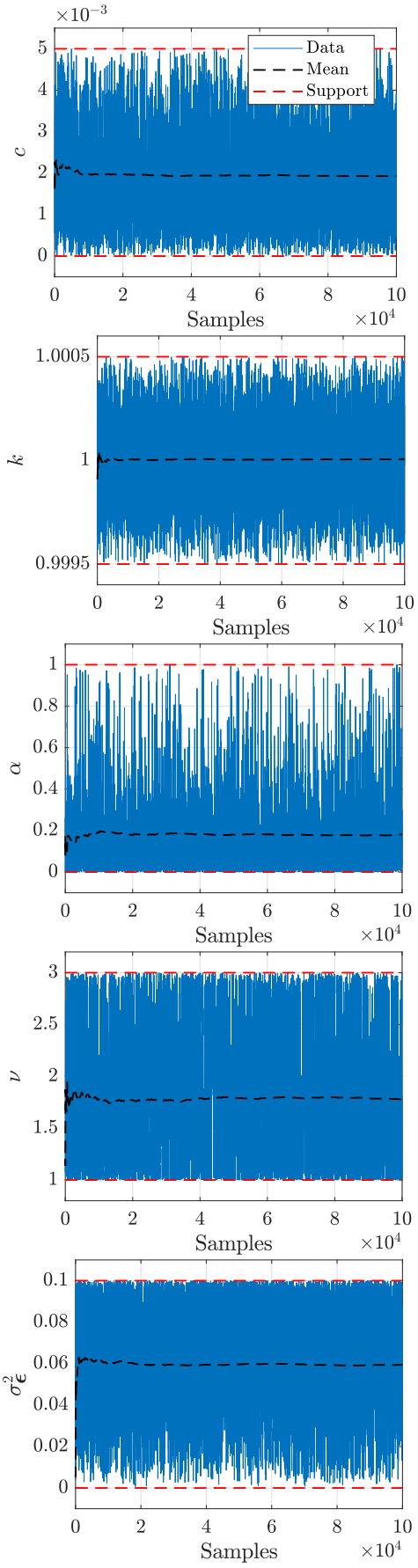

Figure 5. Reduced-order model parameters and discrepancy variance trace plots: $\bar{a} \approx 40\%$. There is no need to burn-in samples.

Table 4. Uniform prior distribution $\mathcal{U}(a, b)$ of the reduced-order model parameters and discrepancy variance for Bayesian inference.

Support	c	k	α	ν	σ^2_{ϵ}
a	0	0.9995	0	1	0
b	0.005	1.0005	1	3	0.1

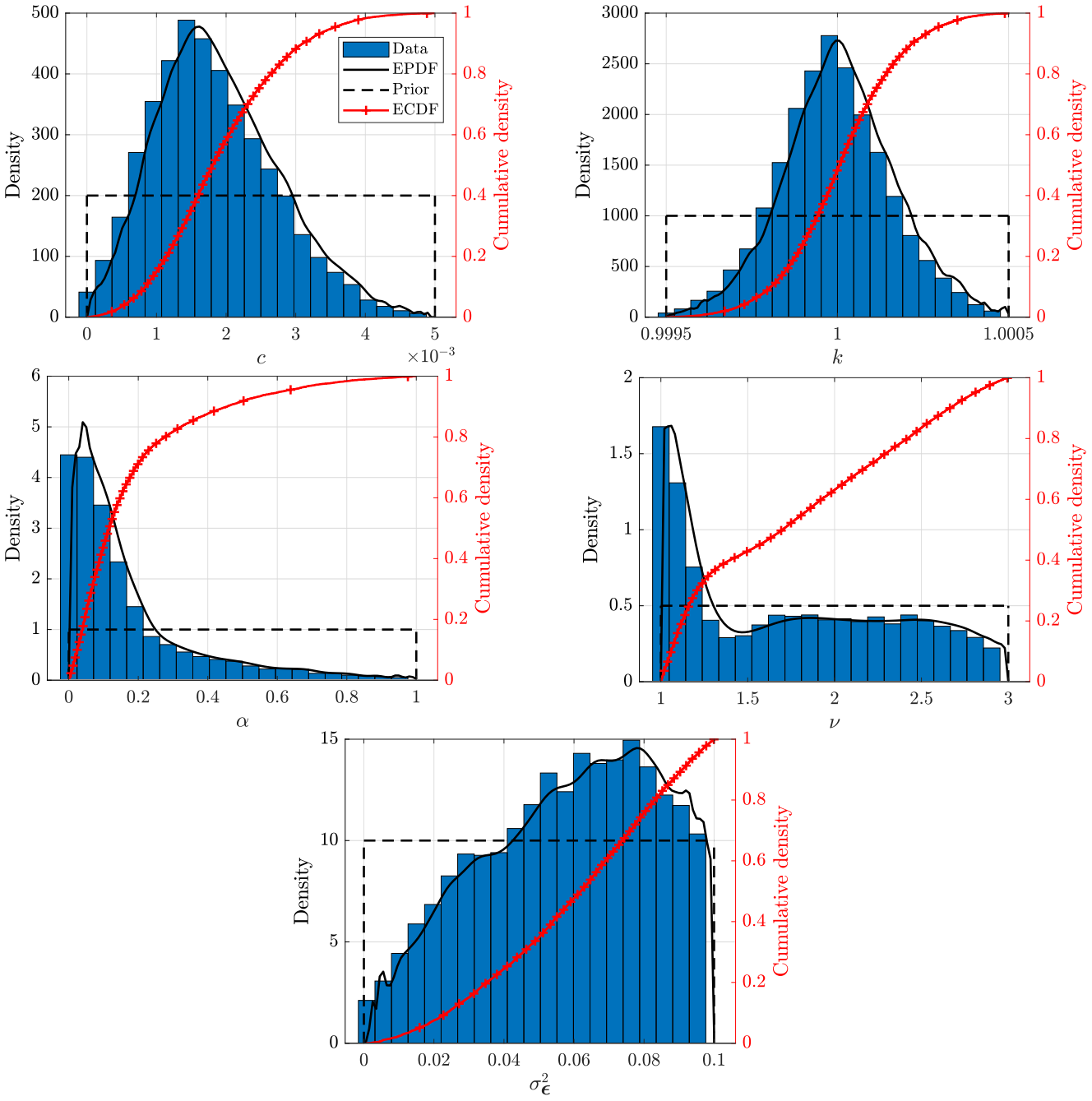

Figure 6. Reduced-order model parameters and discrepancy variance estimated probability density functions (EPDF), Uniform prior distributions and empirical cumulative distribution functions (ECDF).

optimal set of influential parameters using the Cross-Entropy method; 3) estimating the distributions of influential parameters through Bayesian inference. Some parameters of the reduced-order model did not significantly influence the variability of the error metric and were not considered in the calibration procedure. The distributions of the error metrics were estimated, and the reduced-order model is adequate for simulating viscoelastic internal variables for the three initial branches of interest. In addition, the uncertainties were propagated through the viscoelastic internal variable responses, and they are under the data.

Despite some efforts related to the calibration procedure, it guarantees the reduced-order model that best forecasts viscoelastic internal variables. After this process, the reduced-order model could simulate viscoelastic internal variables considering uncertainties with reduced computational cost. Obtaining a robust and cheaper computational model facilitates numerical simulations and research to get more robust

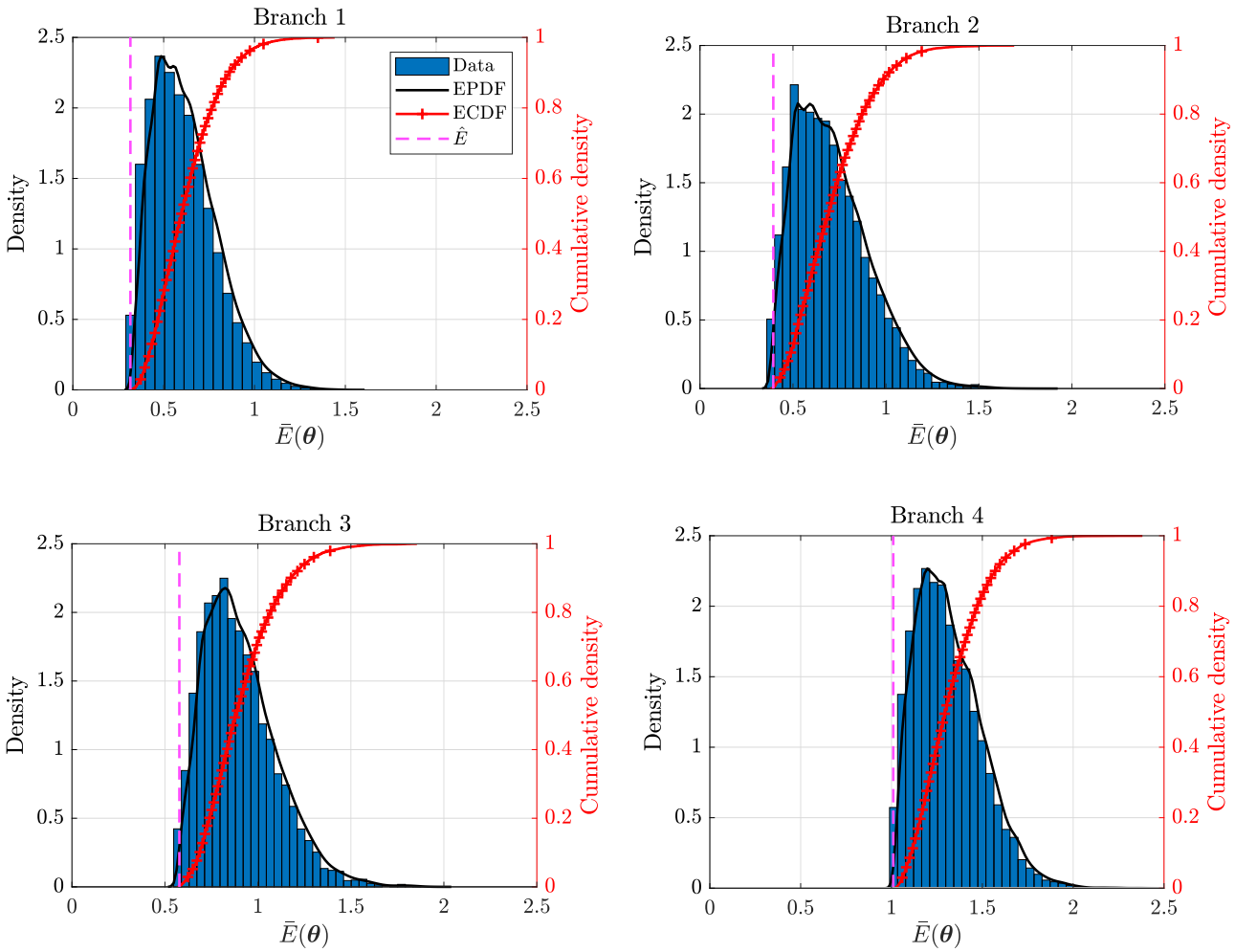

Figure 7. Error measure estimated probability density function (EPDF) and empirical cumulative distribution function (ECDF). The minimum error measure value $\hat{E}$ given by the CE method is indicated.

tires. In this sense, the results of this paper also contribute to the advancement of research on computational models that are more robust and with a reduced computational cost.

Availability of data and material

The MATLAB scripts used in the numerical simulations are available in the following GitHub repository: https://github.com/rafaelraqueti/UQ_Bouc-Wen_calibration.git. The dataset used in this work belongs to Michelin and is not available in this repository.

Acknowledgments

The authors are very grateful to Michelin for providing and trusting the authors with the dataset used in this work. The authors are also thankful for the financial support provided by the Coordination for the Improvement of Higher Education Personnel (CAPES) Grant No. 88887.583012/2020-00.

Funding

The research leading to the results has received funding from CAPES, Grant No. 88887.583012/2020-00; from FAPESP, Grant No. 2016/21973–5 and 2019/19684-3, and CNPq, Grant No. 306526/2019-0.

Declaration of conflicting interests

The authors declared no potential conflicts of interest concerning this article's research, authorship, and publication.

References

Alizadeh R, Allen JK and Mistree F (2020) Managing computational complexity using surrogate models: a critical review. Research in Engineering Design 31(3): 275–298. DOI:10.1007/s00163-020-00336-7.

Botev ZI (2016) The normal law under linear restrictions: simulation and estimation via minimax tilting. arXiv preprint arXiv:1603.04166 .

Brancati R, Strano S and Timpone F (2011) An analytical model of dissipated viscous and hysteretic energy due to interaction forces in a pneumatic tire: Theory and experiments. Mechanical Systems and Signal Processing 25(7): 2785–2795.

Crestaux T, Le Maıˆtre O and Martinez JM (2009) Polynomial-Chaos expansion for sensitivity analysis. Reliability Engineering & System Safety 94(7): 1161–1172. DOI:10.1016/j.ress.2008.10.008. Special Issue on Sensitivity Analysis.

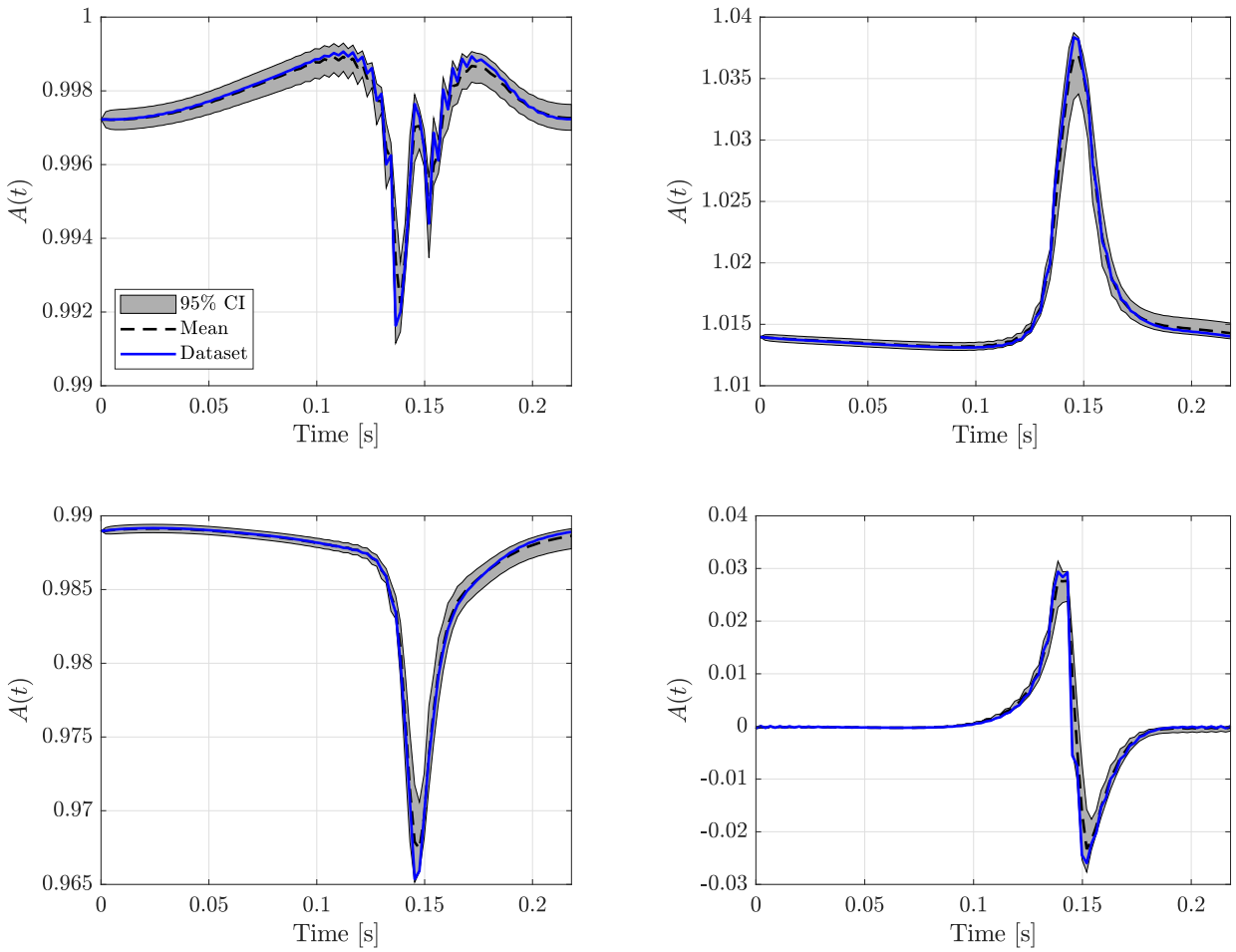

Figure 8. Reduced-order model responses related to different inputs $C(t)$ and initial conditions $A|_{t=0}$, where ■ is the 95% confidence interval (CI), −− the reduced-order model mean and – the viscoelastic internal variable from the dataset.

Cunha A (2021) Enhancing the performance of a bistable energy harvesting device via the cross-entropy method. Nonlinear Dynamics 103(1): 137–155.

De Boer PT, Kroese DP, Mannor S and Rubinstein RY (2005) A tutorial on the cross-entropy method. Annals of operations research 134(1): 19–67.

Fancello E, Stainier L and JPP (2006) A variational formulation of constitutive models and updates in non-linear finite viscoelasticity. International Journal for Numerical Methods in Engineering 65(11): 1831–1864.

Gelman A, Carlin JB, Stern HS, Dunson DB, Vehtari A and Rubin DB (2013) Bayesian data analysis. CRC press.

Ghoreishy MHR (2008) A State of the Art Review of the Finite Element Modelling of Rolling Tyres. Iranian Polymer Journal 17(8): 571–597.

Hall DE and Moreland JC (2001) Fundamentals of rolling resistance. Rubber chemistry and technology 74(3): 525–539.

Homma T and Saltelli A (1996) Importance measures in global sensitivity analysis of nonlinear models. Reliability Engineering and System Safety 52(1): 1–17. DOI:10.1016/0951-8320(96)00002-6.

Hyndman RJ and Koehler AB (2006) Another look at measures of forecast accuracy. International journal of forecasting 22(4): 679–688.

Ismail M, Ikhouane F and Rodellar J (2009) The hysteresis Bouc-Wen model, a survey. Archives of Computational Methods in Engineering 16(2): 161–188.

Jiang K, Wen J, Han Q and Du X (2020) Identification of nonlinear hysteretic systems using sequence model-based optimization. Structural Control and Health Monitoring 27(4): e2500. DOI: 10.1002/stc.2500.

Kroese D, Taimre T and Botev Z (2011) Handbook of Monte Carlo Methods. Wiley Series in Probability and Statistics. Wiley. ISBN 9780470177938. URL https://books.google.fr/books?id=-j3bmyGXKUIC.

Kroese DP, Rubinstein RY and Glynn PW (2013) The cross-entropy method for estimation. In: Handbook of Statistics, volume 31. Elsevier, pp. 19–34.

Le Tallec P and Rahler C (1994) Numerical models of steady rolling for non-linear viscoelastic structures in finite deformations. International journal for numerical methods in engineering 37(7): 1159–1186.

Marelli S, Lüthen N and Sudret B (2021) UQLab user manual – Polynomial chaos expansions. Technical report, Chair of Risk, Safety and Uncertainty Quantification, ETH Zurich, Switzerland. Report # UQLab-V1.4-104.

Miguel LP, Teloli RO and da Silva S (2022) Bayesian model identification through Harmonic Balance Method for hysteresis prediction in bolted joints. Nonlinear Dynamics 107(1): 77–98.

DOI:https://doi.org/10.1007/s11071-021-06967-2.

Oroumiyeh F and Zhu Y (2021) Brake and tire particles measured from on-road vehicles: Effects of vehicle mass and braking intensity. Atmospheric Environment: X 12: 100121. DOI: 10.1016/j.aeaoa.2021.100121.

Pacejka H (2012) Tire and Vehicle Dynamics. 3rd edition. Elsevier Science Technology. ISBN 0080970168. URL https://www.ebook.de/de/product/18341528/hans_professor_of_vehicle_engineering_at_the_delft_university_of_technology_editor_in_chief_of_the_journal_vehicle_system_dynamics_secretary_general_and_president_of_the_international_asso_pacejka_tire_and_vehicle_dynamics.html.

Palar PS, Zuhal LR, Shimoyama K and Tsuchiya T (2018) Global sensitivity analysis via multi-fidelity Polynomial-Chaos expansion. Reliability Engineering & System Safety 170: 175–190. DOI:10.1016/j.ress.2017.10.013.

Real FF, Batou A, Ritto TG and Desceliers C (2019) Stochastic modeling for hysteretic bit–rock interaction of a drill string under torsional vibrations. Journal of Vibration and Control 25(10): 1663–1672. DOI:10.1177/1077546319828245. URL https://doi.org/10.1177/1077546319828245.

Rubinstein RY and Kroese DP (2013) The Cross-Entropy Method: A Unified Approach to Combinatorial Optimization, Monte-Carlo Simulation and Machine Learning. Springer Science & Business Media.

Saadi HA, Ykhlef F and Guessoum A (2011) Mcmc for parameters estimation by bayesian approach. In: Eighth International Multi-Conference on Systems, Signals & Devices. IEEE, pp. 1–6. DOI:10.1109/SSD.2011.5767395.

Segalman DJ (2005) A Four-Parameter Iwan Model for Lap-Type Joints. Journal of Applied Mechanics 72(5): 752–760. DOI: 10.1115/1.1989354. URL https://doi.org/10.1115/1.1989354.

Sobol IM (1993) Sensitivity estimates for nonlinear mathematical models. Mathematical and Computer Modelling 1: 407–414.

Sudret B (2008) Global sensitivity analysis using polynomial chaos expansions. Reliability Engineering & System Safety 93(7): 964–979. DOI:10.1016/j.ress.2007.04.002. Bayesian Networks in Dependability.

Sullivan CC, Yamashita H and Sugiyama H (2022) Reduced Order Modeling of Deformable Tire-Soil Interaction With Proper Orthogonal Decomposition. Journal of Computational and Nonlinear Dynamics 17(5). DOI:10.1115/1.4053592.

Teloli RO, Butaud P, Chevallier G and da Silva S (2022) Good practices for designing and experimental testing of dynamically excited jointed structures: The Orion beam. Mechanical Systems and Signal Processing 163: 108172. DOI:https://doi.org/10.1016/j.ymssp.2021.108172. URL https://www.sciencedirect.com/science/article/pii/S0888327021005495.

Teloli RO, da Silva S, Ritto TG and Chevallier G (2021) Bayesian model identification of higher-order frequency response functions for structures assembled by bolted joints. Mechanical Systems and Signal Processing 151: 107333. DOI:https://doi.org/10.1016/j.ymssp.2020.107333. URL https://www.sciencedirect.com/science/article/pii/S0888327020307196.

Tonegawa Y and Sasaki S (2021) Development of tire-wear particle emission measurements for passenger vehicles. Emission Control Science and Technology 7(1): 56–62.

Walter JD and Conant FS (1974) Energy Losses in Tires. Tire Science and Technology 2(4): 235–260.